Advances in Brief

Sparse Initial Entrapment of Systemically Injected *Salmonella typhimurium* Leads to Heterogeneous Accumulation within Tumors[1]

Neil S. Forbes,[2] Lance L. Munn, Dai Fukumura, and Rakesh K. Jain[3]

E. L. Steele Laboratory, Department of Radiation Oncology, Massachusetts General Hospital and Harvard Medical School, Boston, Massachusetts 02114

Abstract

Blood-borne therapeutics, which rely on diffusion and convection for delivery, often do not accumulate in effective concentrations distant from vasculature and are therefore unable to eradicate all cells within a tumor. Motile bacteria have the potential to overcome the diffusion and pressure gradients that prevent passive materials from penetrating into poorly perfused regions of tumors. Here, we test several proposed mechanisms of *Salmonella typhimurium* accumulation in tumors, including: (*a*) entrapment in the chaotic vasculature of tumors; (*b*) attraction to specific tumor microenvironments; and (*c*) preferential replication within specific microenvironments. After systemic injection of *S. typhimurium* into tumor-bearing mice, we used intravital microscopy and histological techniques to quantify their interaction with tumor vasculature. Immediately after injection, few *S. typhimurium* (<4 in 10,000) adhered to tumor vasculature; most remained passively suspended in the blood. Despite this low initial adhesion, ~10,000-fold more *S. typhimurium* accumulated in tumors than any other organ 1 week after the injection, thus demonstrating their specificity. However, within the tumors, we found that most bacteria were located in necrotic tissue as large colonies far (750 μm) from functional vasculature. Together, these results suggest that *S. typhimurium* has limited ability to adhere to tumor vasculature and migrate within tumors and only survives in tissue that becomes necrotic. Although *S. typhimurium* is a promising delivery vehicle because of its tumor specificity, increasing its intra-tumoral motility should improve its therapeutic effectiveness.

Introduction

Bacteria have been investigated as therapeutic agents for tumors for ~150 years (1). A resurgence of interest in nonpathogenic bacteria as drug delivery vehicles (2–5) and tumoricidal agents (6, 7) has been induced by recent advances in molecular biology, including removal of their toxic genes (7–9) and complete sequencing of their genomes (10, 11). These microbes also have the potential to overcome many of the delivery barriers that hinder conventional chemotherapeutics (12).

Recently, Low *et al.* (8, 13) developed a strain of *Salmonella typhimurium* (VNP20009) that is nonpathogenic in mice, pigs, and humans and accumulates 2000-fold more in tumors than in other organs. However, this strain was not successful at slowing tumor growth in the clinic (13), which prompts the question of how these bacteria are delivered to and specifically replicate within tumors. Obligate anaerobes (*e.g.,* clostridium and bifidobacterium) target the necrotic region of tumors because they can only replicate in the oxygen-free environment found there (2, 7, 14). However, salmonella are facultative anaerobes, able to live in both the presence and absence of oxygen.

We propose four possible mechanisms that may contribute to salmonella accumulation in tumors: (*a*) after injection, *S. typhimurium* becomes trapped in the tortuous and chaotic vasculature typical of tumors; (*b*) the limited circulation in tumors and tumor necrosis protects *S. typhimurium* from macrophages and clearance by the immune system; (*c*) *S. typhimurium* are attracted to specific microenvironments within tumors; and (*d*) *S. typhimurium* preferentially replicate within specific tumor microenvironments.

Using *in vitro* and *in vivo* approaches, we have addressed the question of which of these mechanisms contribute to tumor-specific accumulation of *S. typhimurium*. We used a novel *in vitro* tumor model, tumor cylindroids, to observe bacterial penetration into solid masses of tumor cells. We then used intravital microscopy and the dorsal skin-fold chamber tumor model (15) to measure the distribution and adhesion of *S. typhimurium* to tumor vasculature immediately after injection. The accumulation of *S. typhimurium* was assessed in various organs, and histological sections were prepared to identify the location of accumulated bacteria relative to tumor vasculature. Our results suggest that very few *S. typhimurium* are capable of adhering to tumor vasculature and that they generally grow as large isolated colonies within necrotic regions. These results may explain the limited success of the clinical trials to date.

Materials and Methods

Bacterial Culture. Three strains of *S. typhimurium* were grown in LB[4] broth and on agar plates using standard procedures. SL1344 and the GFP-expressing pSMC21 were a kind gift of Dr. Fred Ausubel, Massachusetts General Hospital and Harvard Medical School; SL7207 was a kind gift of Dr. Bruce Stocker, Stanford Medical School; VNP20009 was provided by Vion Corp. (New Haven, CT). SL7207 is an *AroA*⁻ mutant that is less pathogenic in mice than wild-type SL1344 (16) and is currently being investigated as a tumoricidal agent (5). VNP20009 is a *msbB*⁻ and *purI*⁻ mutant that was specifically developed as a nonpathogenic, tumoricidal agent (8).

Both SL7207 and VNP 20009 were transfected with pSMC21 by electroporation: 25 μF, 400 Ω, and 2.4 kV, using 0.2 cm cuvettes. After transfection, all strains were immediately frozen in LB with 10% glycerol and subsequently maintained in culture with 250 μg/mg kanamycin.

Before injection, all strains were grown overnight in LB from single colonies on fresh agar plates, subcultured 1 in 10, grown to an OD_{620} of 0.5–0.7, centrifuged at 3700 rpm (3200 × *g*) for 10 min, and resuspended in sterile PBS.

Mammalian Cell Culture. LS174T colon carcinoma cells were grown at 37°C, 5% CO_2 in DMEM with 10% fetal bovine serum. Tumor cylindroids were formed by constraining spheroids between two parallel horizontal surfaces with a defined spacing of 150 μm (Fig. 1A). Cell aggregates were grown in tissue culture flasks coated with 0.5 mg/cm² methacrylate (polyheme) for 1 week to form spheroids. Individual spheroids, 300–400 μm in diameter, were then transferred to 96-well plates, and a polycarbonate lid with protruding cylindrical pins (±25 μm in length and 3 mm in diameter) was lowered onto

[4] The abbreviations used are: LB, Luria-Bertani; CFU, colony-forming unit; GFP, green fluorescence protein; SCID, severe combined immunodeficient.
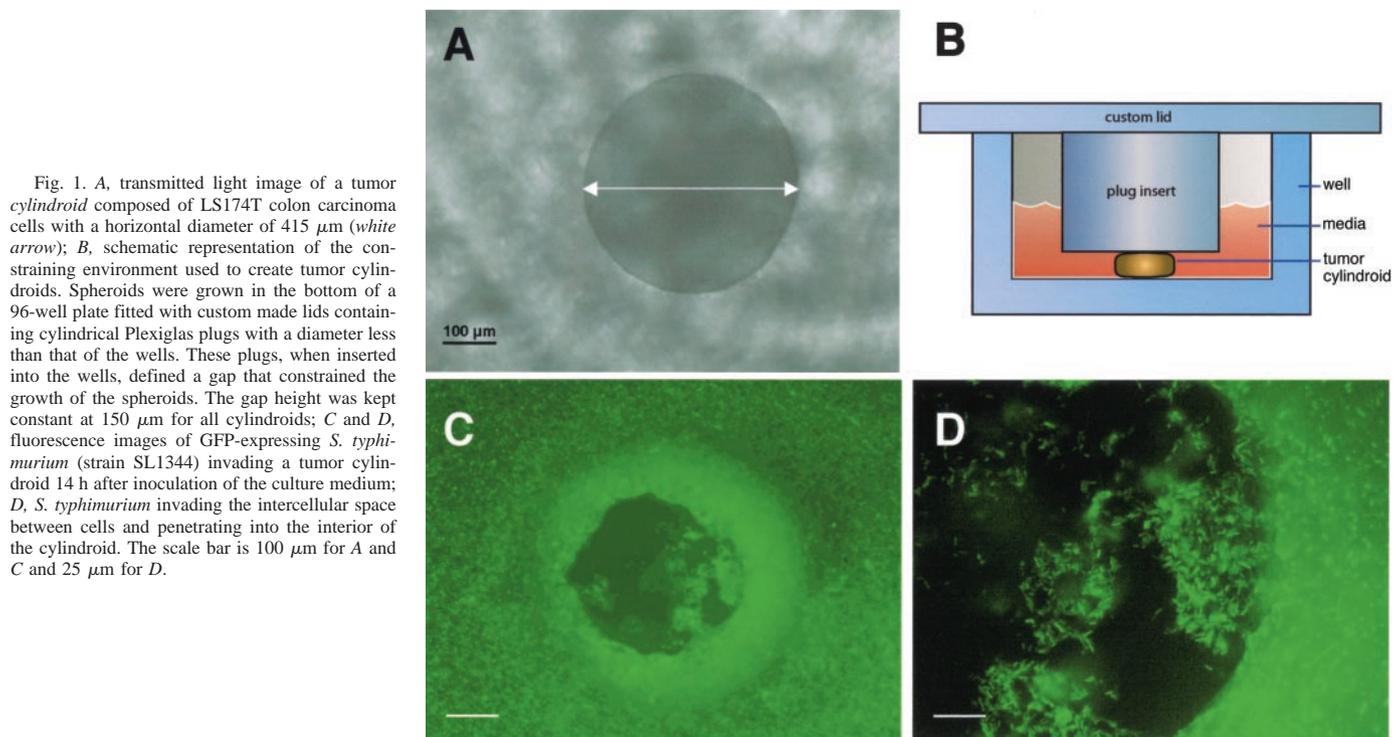
Fig. 1. *A*, transmitted light image of a tumor *cylindroid* composed of LS174T colon carcinoma cells with a horizontal diameter of 415 μm (*white arrow*); *B*, schematic representation of the constraining environment used to create tumor cylindroids. Spheroids were grown in the bottom of a 96-well plate fitted with custom made lids containing cylindrical Plexiglas plugs with a diameter less than that of the wells. These plugs, when inserted into the wells, defined a gap that constrained the growth of the spheroids. The gap height was kept constant at 150 μm for all cylindroids; *C* and *D*, fluorescence images of GFP-expressing *S. typhimurium* (strain SL1344) invading a tumor cylindroid 14 h after inoculation of the culture medium; *D, S. typhimurium* invading the intercellular space between cells and penetrating into the interior of the cylindroid. The scale bar is 100 μm for *A* and *C* and 25 μm for *D*.

the spheroids (Fig. 1*B*). Cylindroids were allowed to equilibrate for 24 h before injection of bacteria into the culture medium (final concentration of 1000 CFU/ml) through holes in the polycarbonate lid. Intratumor cylindroid invasion was then monitored microscopically for 24 h.

Animal Model. Dorsal skinfold chambers were surgically implanted into either SCID mice or immuno-competent C3H mice (male, ~30 grams of body weight), under anesthesia (90 mg of ketamine/10 mg of xylazine per kg body weight), as described previously (15). After a 2-day recovery period, small pieces (~1 mm^3) of MCaIV murine mammary carcinomas were implanted into the chambers. Tumors were monitored through glass coverslips in the dorsal skin fold chambers (15). Intravital bacterial delivery experiments began once the tumors reached an *en face* diameter of 4–7 mm. All procedures were carried out following the Public Health Service Policy on Humane Care of Laboratory Animals and approved by the Institutional Animal Care and Use Committee.

Intravital Microscopy (Measurement of Bacterial Delivery *in Vivo*). Five min before bacteria injection, mice were anesthetized (90 mg of ketamine/10 mg of xylazine/kg body weight) and injected with 0.05 ml of 5 mg/ml rhodamine dextran (2 million molecular weight; Molecular Probes, Eugene, OR) to identify functional vasculature as described previously (17).

Anesthetized mice were restrained and placed on an upright microscope (Zeiss, Göttingen) equipped with an automated stage (Burleigh, Fischer, NY). Four to seven vascularized regions were identified in each tumor depending on their size and extent of vascularization. The automated stage was programmed to return to these locations and cycle between them every 20 or 30 s. Images were acquired through a 20× objective, using a FITC filter set at video-rate using a Hamamatsu CCD camera and a Panasonic S-VHS video tape recorder. After one complete cycle was recorded, bacteria were injected i.v. at either 2 or 20 × 10^6 CFU/mouse suspended in 0.2 ml of sterile PBS.

Quantification of Bacterial Accumulation. One week after bacteria injection, the mice were anesthetized and injected with biotinylated Lycopersicon esculentum (tomato) lectin (5 mg/kg; Vector Laboratories, Burlingame, CA) to identify functional vasculature. After 5 min, the mice were euthanized, and the tumors were extracted and cut in half. One-half of the tumor was fixed in 4% paraformaldehyde and embedded in paraffin. The other half of the tumor and five other extracted organs (liver, spleen, lungs, heart, and abdominal skin) were weighed, minced with scissors, and suspended in sterile PBS. The minced organ suspension was serially diluted and plated on LB agar. Bacterial colonies were counted after overnight incubation at 37°C.

The embedded half of the tumor was cut into 5-μm serial sections. Biotinylated lectins bound to the vasculature were conjugated with Avidin (Vectastain Elite ABC kit) and subsequently visualized with diaminobenzidine according to the manufacturer's recommendation. Successive sections were Brown-Hopps (Gram's stain) stained to identify Gram-negative bacteria.

Statistics. Statistical significance was determined using ANOVA and Fisher's post hoc test. The significance in the slope for the bacterial flux to adhesion comparison was determined using the *F* test for linear regression.

Results

Invasion of *S. typhimurium* into a Three-dimensional Tumor Model *in Vitro*. A three-dimensional tumor model (tumor cylindroids; Fig. 1) was specifically created to observe the invasion of bacteria into tumor tissue. Cylindroids have similar geometric properties to tumor spheroids (18); they contain rapidly proliferating cells in the outer layer, necrotic centers, and a quiescent boundary region (data not shown). However, cylindroids have optically accessible cores and are therefore better suited for microscopically observing the penetration of *S. typhimurium* deep into tissue (>100 μm). In addition, because the interior of cylindroids can be monitored in real time, bacterial motion can be observed within a growing mass of cancer cells.

Fig. 1, *C* and *D* show the extent that *S. typhimurium* invaded into a cylindroid in 14 h. Rapidly swimming *S. typhimuria* were clearly capable of penetrating into tumor cylindroids. During this experiment, bacteria were observed "burrowing" between tumor cells by lining up with the intercellular space and propelling themselves forward (data not shown). These observations demonstrate the ability of *S. typhimurium* to penetrate into a solid mass of tumor tissue and imply that *S. typhimurium* is capable of redistributing within tumors *in vivo*.

Tumor Specificity and Dose Dependence of *S. Typhimurium* Accumulation *in Vivo*. Fig. 2 shows the accumulation of *S. typhimurium* (strain VNP20009) in the organs of mice bearing MCaIV tumors, 1 week after injection. Significantly (>10,000-fold) more bacteria (*P* < 0.0002) accumulated in the tumor than any other organ for C3H mice injected 2 million CFU (Fig. 2, *A* and *B*). The spleen
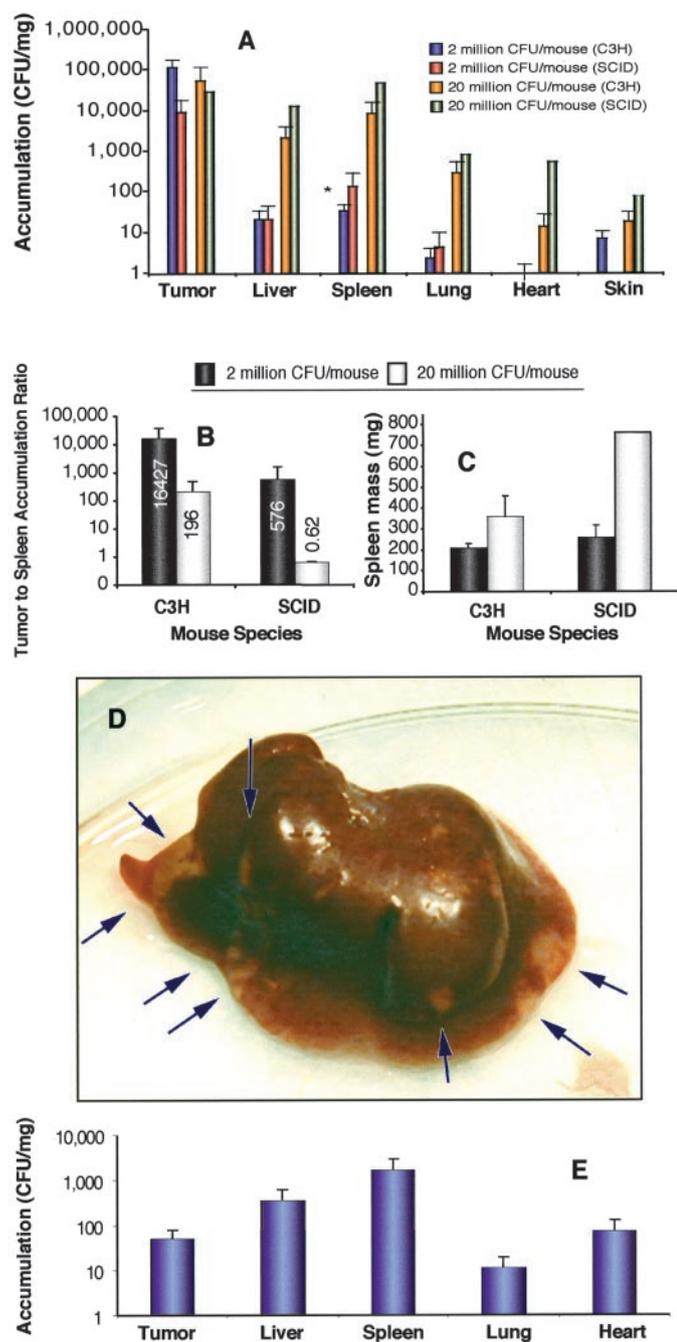
5189

Fig. 2. *A,* accumulation of *S. typhimurium* (strain VNP20009) into the organs of immuno-competent (C3H) and immunodeficient (SCID) mice, both with MCaIV murine mammary carcinomas, 1 week after systemic injection administered at two different doses, 2 million CFU/mouse and 20 million CFU/mouse. Significantly ($P < 0.0002$) more bacteria accumulated in the tumor than any other organ for C3H mice administered 2 million CFU (ANOVA and Fisher's exact test). The spleen, *, accumulated more bacteria than the other organs but significantly less ($P < 0.0002$) than the tumors. For 2 million C3H, 2 million SCID, 20 million C3H, and 20 million SCID, $n = 4, 3, 2,$ and 1 (to show trend), respectively. *B,* ratio of accumulation in the tumor to the accumulation in the spleen in mice injected *S. typhimurium* VNP20009, bearing MCaIV carcinomas; *C,* spleen mass 1 week after bacterial (VNP20009) injection in mice bearing MCaIV carcinomas; *D,* ischemic regions (*white arrows*) in the liver of an immunodeficient SCID mouse that received 20 million CFU. *E,* accumulation of *S. typhimurium*, strain SL7207, in the organs of SCID mice with LS174T colon carcinomas. Significance in all figures was determined using the two-tailed unpaired Student's *t* test; error bars are ±SE.

accumulated more bacteria than the other organs for most of the mice (two had slightly more in the liver). This supports the findings of Low *et al.* (8), who report a tumor accumulation ratio >2000 for this strain of *S. typhimurium* in mice.

The ratio of bacterial accumulation in the tumor to accumulation in the spleen (generally the organ with the greatest accumulation) was strongly dependent on dose (Fig. 2*B*). Surprisingly, mice injected with 20 million CFU accumulated similar numbers of bacteria in tumors compared with the mice injected with 2 million CFU. On the other hand, bacterial accumulation in the other organs increased with dose escalation (Fig. 2*A*). This phenomenon was observed in both immunocompetent C3H mice and immunodeficient SCID mice, indicating that it is not dependent on a fully functional immune system. Either a maximum bacterial growth rate is achieved in tumors or a threshold for clearance is crossed when bacteria can no longer be cleared from normal organs. Low *et al.* (8) also observed that only a narrow dose range could produce significantly large accumulation ratios.

The higher bacteria dose affected the health of the SCID mice; four of five SCID mice did not survive injections of 20 million CFU. The liver of the surviving mouse (Fig. 2*C*) had obvious infarcts, possibly caused by ischemia as a result of bacterial occlusion or aggregates of leukocytes and platelets activated in the presence of the bacteria. The higher dose induced splenomegaly (Fig. 2*D*) in both strains of mice. However, the higher dose did not appear to affect the health of the C3H immunocompetent mice; all survived and were normally active 1 week after the injection.

The accumulation of *S. typhimurium* strain SL7207, which is also currently being investigated as a tumoricidal agent (5), was greater in normal organs than the tumors (Fig. 2*E*). However, SL7207 detrimentally affected the health of the mice. Every mouse had splenomegaly, infarcted livers (similar to Fig. 2*C*), and pungent ascites 1 week after injection with 2 million CFU.

Sparse Adhesion of Bacteria to Tumor Vasculature. The delivery of *S. typhimurium* into MCaIV tumors was observed using intravital microscopy (Fig. 3). After an injection of 20 million CFU, bacteria could clearly be seen flowing in the blood stream in each observed tumor location (Fig. 3*A*). Numerous bacteria were observed (>3.6 bacteria/sec, maximum 9.2 bacteria/sec) in each 0.59 × 0.44 mm field of view. After an injection of 2 million CFU, 10 times fewer bacteria were observed in each location. To determine adhesion events, 20 million CFU bacteria were injected.

No bacteria adhered to the walls of vessels with high flow rates (defined as >~1.5 mm/sec) in any of the 14 mice observed. In vessels with lower flow rates, occasional interactions occurred. Fig. 3, *B–E* show a bacterium adhering; it enters via a small vessel on top of the larger vessels that are more clearly visible in these figures. During 1 h of observation, no qualitative drop in bacterial flux into each field of view was detected. However, no bacteria were detectable in the blood 24 h after injection.

The appearance and disappearance of 106 adherent bacteria were tracked in 23 locations of four mice (Fig. 3*F*). Only bacteria that adhered for >2 min were tracked. Each either dislodged, slowly disappeared, or persisted until the end of observation. Fluorescence of the bacteria may slowly disappear because of photobleaching, bacterial migration, endocytosis, reduced GFP expression, or GFP diffusion through bacterial membranes with increased permeability. Total flux of bacteria into a location was determined by counting all bacteria that entered the field of view over a given period of time. This overall flux represents the sum of all bacterial fluxes through each of the vessels visible in the field. Only $0.035 \pm 0.015\%$ (or <4 in 10,000) of the bacteria that flowed into the tumors permanently adhered (defined as disappearing or persistent bacteria observed for >12 min).

On a *per field* basis, the number of adherent bacteria per time (expressed as rate of adhesion) increased with an increasing overall bacterial flux (Fig. 3*G*; $P < 0.002$). In other words, the more bacteria that flowed into a location, the more that adhered. The dependence in Fig. 3*G* coupled with the observation that bacteria do not adhere to

5190

Fig. 3. *A, S. typhimurium* (strain VNP20009; observed as small *green dots* in the figure) flowing through the vasculature (in *red,* visualized with rhodamine dextran 2 million molecular weight) of a SCID mouse bearing an MCaIV tumor that was administered a dose of 20 million CFU; *B–E,* bacterium observed adhering to tumor vasculature (*white arrows*). The bacterium is not present in *B.* In *C,* the moving bacterium appears as an elongated blur as it enters the focal plane. In *E,* it finally comes to rest in the blood vessel. Each frame (*B–E*) is separated by 33 ms (video rate). This bacterium dislodged from this position after 6 min. The other particles visible in the images are bacteria that adhered previously. *F,* representative history of all bacteria that adhered for >2 min within six locations of an MCaIV tumor in a SCID mouse administered 20 million CFU VNP20009. Bacteria either slowly disappeared (*shaded bars*), were obviously dislodged (terminated *solid bars*), or persisted until the end of observation (*solid bars*). The left end of each bar indicates when the bacterium first adhered. *G,* flux of bacteria into a location significantly ($P < 0.002$) correlated with the number of adherent bacteria that persisted until the end of observation. The scale bars for *A–E* are all 100 μm.
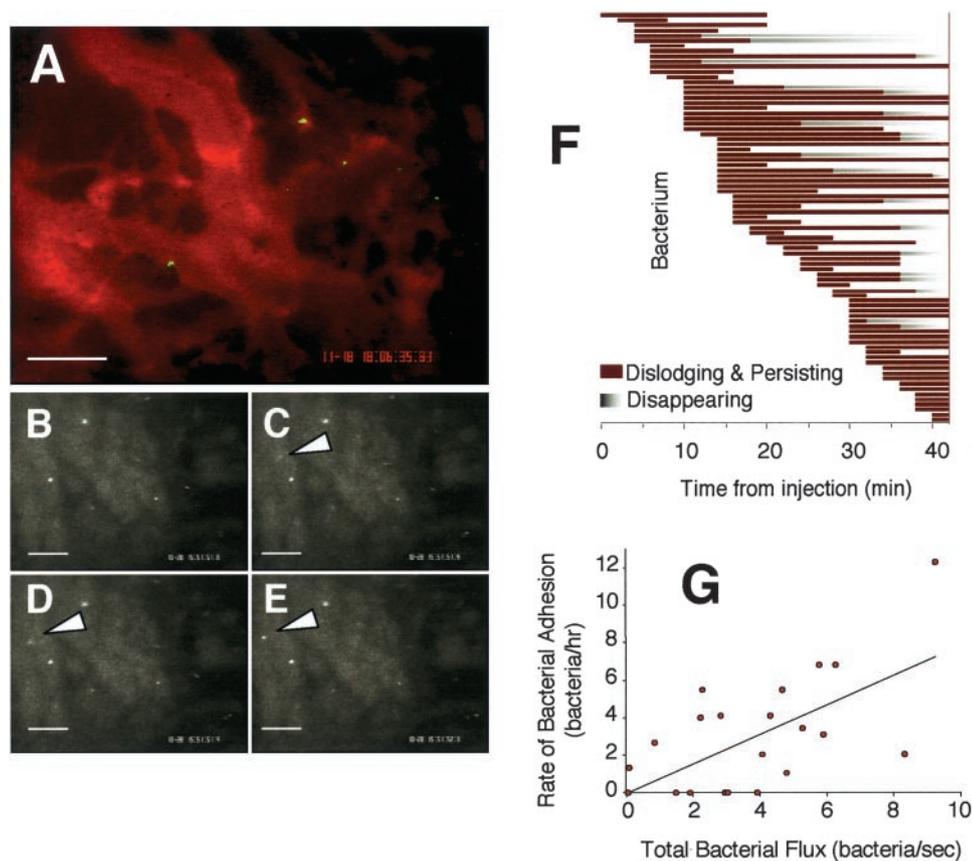
rapidly flowing vessels suggests that bacteria will preferentially adhere (in terms of bacteria per volume) in tissue that contains numerous slow and tortuous vessels, *i.e.,* tumors. Note that the average residence time of dislodged bacteria was 7.6 min.

Colonization of *S. Typhimurium* in the Necrotic Regions of Tumors. The location of bacteria that had accumulated in the tumors was determined by Brown-Hopps staining of transverse sections, cut orthogonally from the coverslip in the dorsal-skin-fold chamber (Fig. 4). The same mice were used for intravital microscopy, quantification of bacterial accumulation, and histological sectioning. For each of the sections, ×100 magnification was used to locate bacteria and identify whether they were in colonies or spread sparsely (Fig. 4, *A–C*). Biotinylated lectin perfusion stained only vessels with active blood flow, allowing identification of functional vasculature. (Fig. 4*E*).

No bacteria were found in the living tumor tissue of any of the mice; they were only present in the necrotic regions (Fig. 4, *A–C*). Bacteria could not be found in smaller tumors that lacked necrosis. Most of the bacteria were found in large colonies (Fig. 4*D*) that occupied a small percentage of the total tumor volume (the sections shown in Fig. 4, *A–C* contained more bacteria than the sections from the other mice). The average distance between the colonies and the functional vasculature was 750 ± 40 μm with a minimum distance of 100 μm.

Discussion

***S. Typhimurium* Localization to Tumor Necrosis.** In our experiments, *S. typhimurium* were injected into tumor-bearing mice systemically. These bacteria were observed flowing through tumor vasculature and adhering sparingly (0.035%; Fig. 3). After 1 week, the bacteria had specifically accumulated within the necrotic regions of the tumors, significantly distant from functional vasculature (Figs. 2 and 4).

There are three possible mechanisms to explain this localization to tumor necrosis. Either (*a*) *S. typhimurium* are specifically attracted to necrotic tissue and migrate there from the vasculature through living tumor tissue; (*b*) *S. typhimurium* adhere sparsely on tumor vasculature, migrate a short distance outside the vessels but only successfully colonize tissue that becomes necrotic; in this case, either the necrotic microenvironment is advantageous for growth or these regions provide shelter from the immune system; or (*c*) *S. typhimurium* occlude tumor vasculature in a similar fashion to the liver infarcts in Fig. 2*C*. Thus, the bacteria never need to leave the blood vessel but survive and colonize in these occluded/dying vessels in tissue soon to become necrotic. This would explain the large distance from functional vasculature and is the subject of future experimentation.

Entropically, it seems implausible that bacteria would migrate to necrotic tissue and congregate in colonies such as those in Fig. 4. If they were attracted to components in necrotic tissue and freely motile, they would most likely spread out to more uniformly consume these components. The stochastic nature of bacterial chemotaxis implies that bacteria migrate toward and consume chemo-attractant, moving on to new sources once consumed, thereby resulting in a more homogeneous distribution than observed. The fact that this did not appear to happen suggests that *S. typhimuria* have limited motility within the tumor, instead surviving only in tissue that becomes necrotic after injection (mechanisms II and III).

***S. Typhimurium* as a Future Therapeutic.** Previously, we suggested the properties of an ideal anticancer bacterium (1). An ideal bacterium would be: (*a*) nontoxic to the host; (*b*) only able to replicate within the tumor; (*c*) motile and able to disperse evenly throughout a tumor; (*d*) slowly and completely eliminated from the host; (*e*) nonimmunogenic; and (*f*) able to cause lysis of tumor cells. Our results suggest that the biggest shortcoming of *S. typhimurium* is its inability to disperse throughout the tumor. Dang *et al.* (7) dramatically dem-
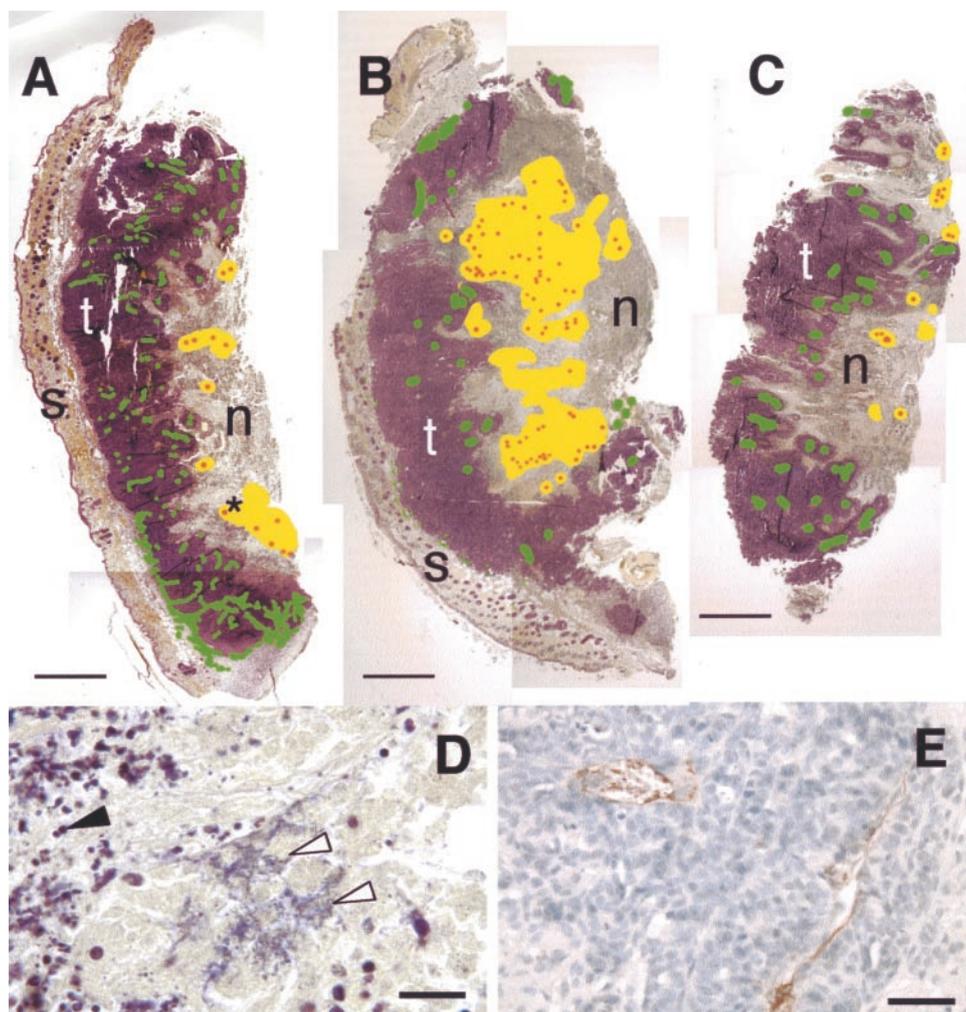
Fig. 4. Tiled reconstructions of histological sections of Brown-Hopps stained s.c. tumors in a C3H mouse administered 20 million CFU (*A*), a C3H mouse administered 2 million CFU (*B*), and a SCID mouse administered 20 million CFU (*C*). The colored regions were identified at ×100 (*red,* location of bacterial colonies; *yellow,* tumor tissue sparsely populated with bacteria; *green,* functional vasculature within the tumor). The labeled regions are *t,* viable tumor tissue (*purple*); *n,* necrotic tumor tissue (*tan*); and *s,* skin. All labeled colonies were densely packed and typically contained >100 individuals. Sparsely populated tissue contained ~1–10 bacteria/290 × 190 μm field of view. No functional vessels were present in the necrotic issue, and no bacteria were detected in the viable tissue. Scale bars are 1 mm. *D,* average-sized bacteria colony (*white arrows*), located at ∗ in *A*. Nuclear debris from dead tumor cells stained purple (*black arrow*). Scale bar is 40 μm. *E,* lectin staining used to identify vessels in *A–C.* Scale bar is 100 μm.

onstrated the importance of this capability by selecting a strain of clostridium (*C. novyi*) able to disperse evenly and eradicating tumors in mice by combining its administration with chemotherapy. An additional strategy would involve modifying the tumor matrix that would facilitate the motility and penetration of the bacteria (19, 20).

Regardless, *S. typhimurium* has a couple of advantages over the obligate anaerobe *C. novyi*. Being a facultative anaerobe, it can be injected active and motile, potentially increasing its tumor specificity. Being a Gram-negative enteric bacterium, similar to *Escherichia coli*, it is far easier to genetically manipulate than any obligate anaerobe.

S. typhimurium was found to aggressively penetrate into three-dimensional cultured tumor tissue *in vitro*. Intravital microscopy demonstrated that <0.04% of *S. typhimurium* that flow into tumors are able to adhere to tumor vasculature. Subsequently, *S. typhimurium* accumulates only in necrotic regions of tumors that are distant from tumor vasculature. These results may explain why tumors were not eradicated in mouse models treated with *S. typhimurium* and the limited success of preliminary clinical trials. Additionally, these results help define the obstacles necessary to overcome for a successful bacteriolytic therapy. An engineered strain of *S. typhimurium* able to disperse more homogeneously throughout a tumor would be a more successful drug delivery or tumoricidal agent. This could potentially be accomplished by genetically inducing matrix-degrading enzymes and/or enhancement of intrinsic motility machinery (19).

Acknowledgments

References

1. Jain, R. K., and Forbes, N. S. Can engineered bacteria help control cancer? Proc. Natl. Acad. Sci. USA, *98:* 14748–14750, 2001.
2. Liu, S. C., Minton, N. P., Giaccia, A. J., and Brown, J. M. Anticancer efficacy of systemically delivered anaerobic bacteria as gene therapy vectors targeting tumor hypoxia/necrosis. Gene Ther., *9:* 291–296, 2002.
3. King, I., Bermudes, D., Lin, S., Belcourt, M., Pike, J., Troy, K., Le, T., Ittensohn, M., Mao, J., Lang, W., Runyan, J. D., Luo, X., Li, Z., and Zheng, L. M. Tumor-targeted salmonella expressing cytosine deaminase as an anticancer agent. Hum. Gene Ther., *13:* 1225–1233, 2002.
4. Nuyts, S., Theys, J., Landuyt, W., van Mellaert, L., Lambin, P., and Anne, J. Increasing specificity of anti-tumor therapy: cytotoxic protein delivery by non-pathogenic clostridia under regulation of radio-induced promoters. Anticancer Res., *21:* 857–861, 2001.
5. Bereta, M. K., Glover, R. T., Hayhurst, A., Wu, A. M., Arakawa, F., and Kaufman, H. L. Construction of a recombinant salmonella vector displaying anti-CEA antibody: a novel method for targeting colon adenocarcinomas. San Francisco: Abstracts for AACR Conference, 2002.
6. Bermudes, D., Zheng, L. M., and King, I. C. Live bacteria as anticancer agents and tumor-selective protein delivery vectors. Curr. Opin. Drug Discov. Devel., *5:* 194–199, 2002.
7. Dang, L. H., Bettegowda, C., Huso, D. L., Kinzler, K. W., and Vogelstein, B. Combination bacteriolytic therapy for the treatment of experimental tumors. Proc. Natl. Acad. Sci. USA, *98:* 15155–15160, 2001.
8. Low, K. B., Ittensohn, M., Le, T., Platt, J., Sodi, S., Amoss, M., Ash, O., Carmichael, E., Chakraborty, A., Fischer, J., Lin, S. L., Luo, X., Miller, S. I., Zheng, L., King, I., Pawelek, J. M., and Bermudes, D. Lipid A mutant Salmonella with suppressed

virulence and TNFalpha induction retain tumor-targeting in vivo. Nat. Biotechnol., *17:* 37–41, 1999.

9. Clairmont, C., Lee, K. C., Pike, J., Ittensohn, M., Low, K. B., Pawelek, J., Bermudes, D., Brecher, S. M., Margitich, D., Turnier, J., Li, Z., Luo, X., King, I., and Zheng, L. M. Biodistribution and genetic stability of the novel antitumor agent VNP20009, a genetically modified strain of Salmonella typhimurium. J. Infect. Dis., *181:* 1996–2002, 2000.

10. McClelland, M., Sanderson, K. E., Spieth, J., Clifton, S. W., Latreille, P., Courtney, L., Porwollik, S., Ali, J., Dante, M., Du, F., Hou, S., Layman, D., Leonard, S., Nguyen, C., Scott, K., Holmes, A., Grewal, N., Mulvaney, E., Ryan, E., Sun, H., Florea, L., Miller, W., Stoneking, T., Nhan, M., Waterston, R., and Wilson, R. K. Complete genome sequence of Salmonella enterica serovar Typhimurium LT2. Nature (Lond.), *413:* 852–856, 2001.

11. Parkhill, J., Dougan, G., James, K. D., Thomson, N. R., Pickard, D., Wain, J., Churcher, C., Mungall, K. L., Bentley, S. D., Holden, M. T., Sebaihia, M., Baker, S., Basham, D., Brooks, K., Chillingworth, T., Connerton, P., Cronin, A., Davis, P., Davies, R. M., Dowd, L., White, N., Farrar, J., Feltwell, T., Hamlin, N., Haque, A., Hien, T. T., Holroyd, S., Jagels, K., Krogh, A., Larsen, T. S., Leather, S., Moule, S., O'Gaora, P., Parry, C., Quail, M., Rutherford, K., Simmonds, M., Skelton, J., Stevens, K., Whitehead, S., and Barrell, B. G. Complete genome sequence of a multiple drug resistant Salmonella enterica serovar Typhi CT18. Nature (Lond.), *413:* 848–852, 2001.

12. Jain, R. K. The next frontier of molecular medicine: delivery of therapeutics. Nat. Med., *4:* 655–657, 1998.

13. Toso, J. F., Gill, V. J., Hwu, P., Marincola, F. M., Restifo, N. P., Schwartzentruber, D. J., Sherry, R. M., Topalian, S. L., Yang, J. C., Stock, F., Freezer, L. J., Morton, K. E., Seipp, C., Haworth, L., Mavroukakis, S., White, D., MacDonald, S., Mao, J., Sznol, M., and Rosenberg, S. A. Phase I study of the intravenous administration of attenuated Salmonella typhimurium to patients with metastatic melanoma. J. Clin. Oncol., *20:* 142–152, 2002.

14. Nuyts, S., Van Mellaert, L., Theys, J., Landuyt, W., Lambin, P., and Anne, J. Clostridium spores for tumor-specific drug delivery. Anticancer Drugs, *13:* 115–125, 2002.

15. Leunig, M., Yuan, F., Menger, M. D., Boucher, Y., Goetz, A. E., Messmer, K., and Jain, R. K. Angiogenesis, microvascular architecture, microhemodynamics, and interstitial fluid pressure during early growth of human adenocarcinoma LS174T in SCID mice. Cancer Res., *52:* 6553–6560, 1992.

16. Hormaeche, C. E., Mastroeni, P., Harrison, J. A., Demarco de Hormaeche, R., Svenson, S., and Stocker, B. A. Protection against oral challenge three months after i. v. immunization of BALB/c mice with live Aro Salmonella typhimurium and Salmonella enteritidis vaccines is serotype (species)-dependent and only partially determined by the main LPS O antigen. Vaccine, *14:* 251–259, 1996.

17. Brown, E. B., Campbell, R. B., Tsuzuki, Y., Xu, L., Carmeliet, P., Fukumura, D., and Jain, R. K. In vivo measurement of gene expression, angiogenesis and physiological function in tumors using multiphoton laser scanning microscopy. Nat. Med., *7:* 864–868, 2001.

18. Sutherland, R. M. Cell and environment interactions in tumor microregions: the multicell spheroid model. Science (Wash. DC), *240:* 177–184, 1988.

19. Brown, E., McKee, T., di Tomaso, E., Seed, B., Boucher, Y., and Jain, R. K. Dynamic imaging of collagen and its modulation in tumors in vivo using second harmonic generation. Nat. Med., *9:* 796–801, 2003.

20. Netti, P. A., Berk, D. A., Swartz, M. A., Grodzinsky, A. J., and Jain, R. K. Role of extracellular matrix assembly in interstitial transport in solid tumors. Cancer Res., *60:* 2497–2503, 2000.

Sparse Initial Entrapment of Systemically Injected *Salmonella typhimurium* Leads to Heterogeneous Accumulation within Tumors

Neil S. Forbes, Lance L. Munn, Dai Fukumura, et al.

Updated version	Access the most recent version of this article at: http://cancerres.aacrjournals.org/content/63/17/5188

Cited articles	This article cites 19 articles, 6 of which you can access for free at: http://cancerres.aacrjournals.org/content/63/17/5188.full#ref-list-1
Citing articles	This article has been cited by 10 HighWire-hosted articles. Access the articles at: http://cancerres.aacrjournals.org/content/63/17/5188.full#related-urls

E-mail alerts	Sign up to receive free email-alerts related to this article or journal.
Reprints and Subscriptions	To order reprints of this article or to subscribe to the journal, contact the AACR Publications Department at pubs@aacr.org.
Permissions	To request permission to re-use all or part of this article, use this link http://cancerres.aacrjournals.org/content/63/17/5188. Click on "Request Permissions" which will take you to the Copyright Clearance Center's (CCC) Rightslink site.